2017 Asia-Pacific Engineering and Technology Conference (APETC 2017)
ISBN: 978-1-60595-443-1

Nano and Submicron Olivine Synthesized by Hydrothermal Process

Masakazu Togo, Shunsuke Yagi and Atsushi Nakahira

ABSTRACT

Development of cobalt free olivine material as a cathode for lithium ion battery was carried out. Especially, in this study, Mn substituted olivine was synthesized by hydrothermal process. With the reaction conditions, such as hydrothermal reaction temperature and times, the morphology and particle size were variable. Under the optimum synthetic condition, finer olivine particle was obtained by hydrothermal process. In addition, the effect of Mn addition on the microstructure of olivine was investigated.

INTRODUCTION

As the sustainable energy resources, green energy such as solar power is a promising energy source, but tends to depend on the weather. In order to supply steady energy, the technical development of energy storage is needed. Lithium ion battery (LIB) has the best energy density in the secondary battery and is efficient for the energy storage about larger capacity. Therefore, LIB has contributed to the miniaturization of the devices. In order to storage more energy, a larger amount of battery are needed, so the selectivity of the composed material is significantly important. Lithium cobalt oxide (LCO) is used as cathode material for 4V class cathode with the capacity of about 150mAh/g. Because the usable capacity caused by exhausting only a half lithium ion in the structure is limited, the attempts of ceramics coating such as zirconia to LCO particle has been reported. [1] Nowadays, on the other hands, cobalt-free cathode is needed, because cobalt is rare and expensive from the view point of adopting for large battery and mass production. Spinel-type lithium manganese oxide (LMO) and olivine-type lithium iron phosphate (LFP) have also attracted increasing attention as a cathode material. These redox species, Fe or Mn, is abundant material, so these battery is cheaper than LCO. In special, LFP with higher stabilities is expected to be applicable as a long-life battery.

LFP belongs to polyanion cathode material, and its working voltage is about 3.5V v.s. Li higher than the other iron phosphates. [2] The crystal structure is classified to

Masakazu Togo[1,a], Shunsuke Yagi[2,b] and Atsushi Nakahira[1,c]
[1]Osaka Prefecture University, BldgB5, 3B-31, 1-1 Gakuen-cho, Naka-ku, Sakai, 599-8531, Japan
[2]The University of Tokyo, Institute of Industrial Science Fw403, 4-6-1 Komaba, Meguro-ku, Tokyo, 153-8505, Japan
[a]st110029@edu.osakafu-u.ac.jp[1], [b]syagi@iis.u-tokyo.ac.jp, [c]nakahira@mtr.osakafu-u.ac.jp
[1] * Corresponding author:st110029@edu.osakafu-u.ac.jp

space group Pnma, and PO_4 tetrahedral and FeO_6 octahedral is edge-shearing. At high temperature, separation of oxygen from the olivine structure is a little because of the strong covalent bond between P and O, so the stability is better than other materials. In charge-discharge process, the reaction is showed following Eq. 1:

$$LiFePO_4 \Leftrightarrow Li^+ + e^- + FePO_4 \quad \text{Eq.(1)}$$

Two phases for $LiFePO_4$ and $FePO_4$ has the similar $FePO_4$ unit structure, and the unit structure has not changed before and after reaction. Then, the degradation of the capacity for $LiFePO_4$ is small. On the other hand, LFP has the insulation property as well as the most of polyanion materials. The conductivity of LCO is about 10^{-2}S/cm, but that of LFP is ~10^{-8}S/cm. [3] In order to improve its conductivity of LFP, the addition of conductive material has tried. For example, carbon as electronic conductive layer is coated to olivine particle surface by mixing with polymer and sintering under vacuum or reducing atmosphere. [4] As an ion conductive layer, amorphous Li_3PO_4 is coated by solid state reaction. [5] These coated material show better electric properties at high rate. However, in the case of increasing thickness of coating layer, the real energy density of cathode material decrease.

In order to enhance the electrode property, substitution or doping another element is efficient. In olivine material, the improvement of electric conductivity has been reported due to doping multiply-charged ion such as Mg^{2+}, Al^{3+}, Ti^{4+}, Nb^{5+}, and W^{6+}.[6] Zr substitution is efficient to prevent the degradation of capacity. [7] As the other redox species, manganese has lower potential than iron. Addition of manganese is expected to expand the potential of olivine v.s. Li. In the olivine structure, Mn^{2+}, Co^{2+}, and Ni^{2+} can substitute to Fe^{2+} sites. Therefore, Mn substituted Fe olivine is focused in this study. Herein, the synthesis method is carried out by solid state[8], mechano chemical[9], sol-gel[10], and hydrothermal process.[11] A. Yamada et. al. optimized the temperature of synthesizing olivine by solid state reaction, but high temperature about 893K and long reaction time were needed.[12] Solution process has the advantages of synthesis of homogeneous compound, and reaction condition is mild, relatively. In addition, it is easy to control the morphology, and various results about morphology has reported by sol-gel, hydrothermal, and solvothermal process. [13][14][15] It is efficient that morphology control such as the decrease of the particle size can lead to the improvement of the conductivity cased by shortening the Li ion conduction pass.

In this study, Mn substituted $LiFePO_4$ with fine particle size was synthesized by hydrothermal process. Effect of Mn-substitution on the crystal structure, the local structure around Mn and Fe was examined. The microstructure and other properties were investigated.

EXPERIMENTAL PROCEDURE

$LiOH\text{-}H_2O$, $(NH_4)_2HPO_4$, $FeSO_4\text{-}7H_2O$, $MnSO_4\text{-}5H_2O$ were used as starting materials. These reagents were weighted with molar ratio Li : P : Fe : Mn = 2 : 1 : 1-x : x (x = 0 and 0.25), respectively. In order to prevent the oxidation of Fe^{2+} to Fe^{3+}, distilled water was bubbled by N_2 gas, and the synthesis was done under N_2 atmosphere. After measurement, reagents were put into distilled water in Teflon vessel and vigorously mixed for few minutes. Teflon vessel with dissolved solution was hydrothermally treated at 473 K for 12 hours. Obtained products were filtrated,

washed, and dried under vacuum for overnight. The crystal phase of samples was identified by XRD (Ultima IV, Rigaku Co., Japan) at 2 θ = 10-60° with scan rate of 4°/min using Cu Kα radiation. In order to estimate the lattice constants, internal reference method was used using pure silicon. The morphology was observed by FE-SEM (S-4500, Hitachi, Japan) with applied voltage of 10 kV. The specific surface area was measured by BET method using the data of $P/P_0 = 10^{-3}$-10^{-2}. The local structure of samples was investigated by XAFS spectra for Fe *K*-edge and Mn *K*-edge. XAFS data were corrected by transmission mode using Si (111) double crystal monochrometer at BL14B2 in the SPring-8. For the XAFS measurement, the samples was prepared as pellets with the thickness varied to obtain a 0.5-1.0 jump at the both Fe *K*-edge and Mn *K*-edge. The evaluation of XAFS data was conducted using the commercial software "REX2000" (Rigaku Co.Ltd., Japan).

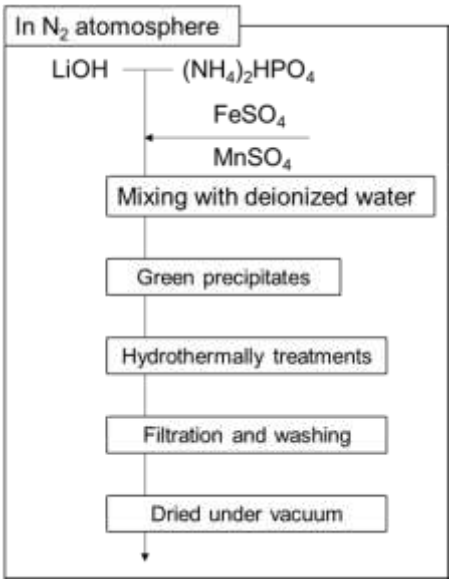

Figure 1. Synthesis flow.

RESULTS AND DISCUSSION

Reaction Temperature

In order to synthesize olivine with no Mn addition, reaction temperatures were changed from 393K to 493K. Fig.2 shows XRD results of products without Mn addition synthesized by hydrothermal process at various hydrothermal reaction temperatures. For samples synthesized at 393K, the peak of 10° was attributed to the layered structure compound for iron phosphate. XRD results for samples synthesized over 423K showed that the diffraction peaks were attributed to the olivine-type structure (JCPDS #83-2092), and the secondary phase such as FeO(OH) and Li_3PO_4 was not observed. Thus, the products synthesized at from 423K to 493K were identified as the monophase of olivine.

In addition, the crystallite size estimated by Scherrer equation was about 57.1nm for all products without Mn addition synthesized by hydrothermal process at various temperatures, independed on the hydrothermal reaction temperatures. SEM images

were showed in Fig.3. At 423K, a particle size was about 300nm and shapes was strip-like. With increasing the reaction temperature, a particle size was increasing to about 0.8 μ m and shapes was strip-like and in part plate-like particle. In the hydrothermal process, reaction temperature attracted to nucleation and particle growth of olivine phase. On the other hand, Chen et al. reoprted that Fe/Li increases especially under 453K of hydrothermal temperature, led to the decrease of conductivity.[16] Therefore the reaction at higher temperature is favorite for olivine-type structure. In this study, olivine was synthesized at 473K as optimum reaction temperature.

Reaction time

Next, the effect of reaction time on the microsturctures of olivine was studied. The products was synthesized at 473K for 1~72h. XRD patterns and SEM images were showed in Fig.4.and Fig.5, respectively. For all products synthesized at 473K for all reaction times, the diffraction peaks of products was attributed to olivine-type structure, and the secondary phase was not observed. The crystallite size was about 58.3nm, and monophase for olivine phase was obtained. Therefore, the effect of reaction time on the crystal structure was not remarkable. From SEM images of products synthesized at 473K for 1h, the particle size was about 20~50nm and morphology was granular. In contrast, for 72h, the size was mainly over 1 μ m and the particle under 100nm was partly observed, and the morphology was plate-like. Then, the growth of olivine was observed with increasing the reaction time. In this study, it is suggested that the reaction times had an influence on the morphology, not the crystal structure.

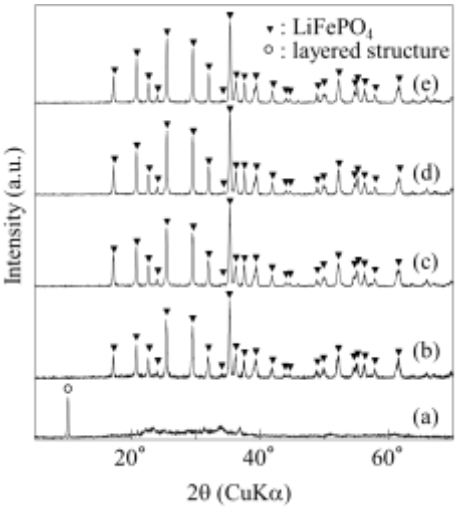

Figure 2. XRD patterns of the products synthesized by hydrothermal process at various temperature for 24h.
(a) 393K, (b)423K, (c)443K, (d)473K, and (e)493K

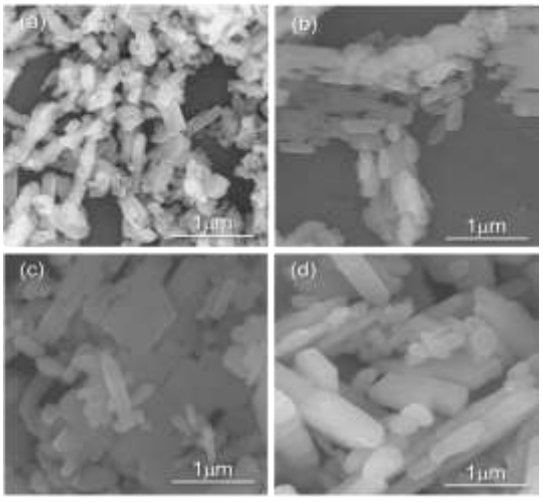

Figure 3. SEM images of the products synthesized by hydrothermal process at various temperature for 24h.
(a) 423K, (b)443K, (c)473K, and (d)493K

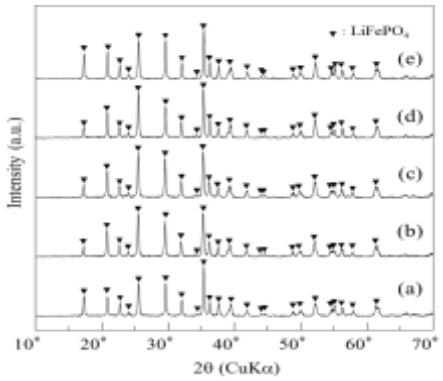

Figure 4. XRD patterns of the products synthesized by hydrothermal process at 473K for 1~72h. (a) 1h, (b)3h, (c)6h, (d)12h, and (e)72h

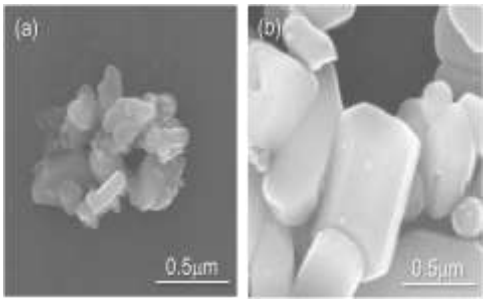

5. SEM images of the products synthesized by hydrothermal process at 473K for 1~72h.. (a) 1h, and (b)72h.

Mn-substitution

Synthesis of Mn-substituted olivines were attempted by hydrothermal treatments at 473K. Mn was added to olivine with the ration of Mn/Fe=25/75(x=0.25). XRD patterns of Mn added products synthesized by hydrothermal process are showed in Fig. 6. The diffraction peaks were attributed to olivine-structure, without the secondary phase estimated as Mn compounds. Compared to products without Mn addition, the peaks were shifted to low-angle from the expansion of lattice spacing. Herein, the radius of Mn^{2+} ion (0.83Å) is larger than that of Fe^{2+} ion (0.61Å). Therefore, this expansion of lattice spacing was thought to be caused by Mn substitution with Fe site in olivine structure. Actually, the estimated unit cell volume with x=0 and 0.25 was 291.3$Å^3$ and 294.4$Å^3$, respectively, the enlargement of unit cell for Mn-substituted olivine. In this study, unit cell volume of the samples synthesized by hydrothermal process at 473 K was 291.3 $Å^3$. Unit cell volume of $LiFePO_4$ was depended on the hydrothermal reaction temperature, typically. In 291.4±0.2 $Å^3$ of the unit cell volume, better electric chemical property was obtained. [17]

SEM images of the Mn added samples synthesized by hydrothermal process are shown in Fig.6. Although olivine with x=0 had the plate like molphology less than 500nm, in case of olivines with Mn addition, their morphologies were changed from plate-like particle to strip-like with a little larger aspect ratio than the products in x=0. Specific surface area by BET method was about 7.2 m^2/g respectively, and the particle size estimated from specific surface area was about 250nm, which agreed well with SEM results. Therefore, nano and submicron sized Mn-substituted olivines were successfully obtained by hydrothermal treatments for the optimum reaction times.

FT-IR spectra was showed in Fig. 7. According to A. Rulmont et al., IR spectra of PO_4 tetrahedral was attributed in following.[18] In x=0, υ_1 symmetric stretching vibration of P-O was 985.3 cm^{-1}, and υ_3 asymmetric stretching vibrations were

1053.4, 1095.9 and 1138.4 cm^{-1}. In addition, υ_2 symmetric bending of O-P-O was 474.9 cm^{-1}, and υ_4 asymmetric bending was 501.9, 552.9, 578.4 and 635.1 cm^{-1}. With Mn addition, one of absorption band was shifted to blue shift, for example υ_1 of x=0.25 sample was shifted to 998.1 cm^{-1}. This shows the possibility that bonding between P and O was affected by Mn addition.

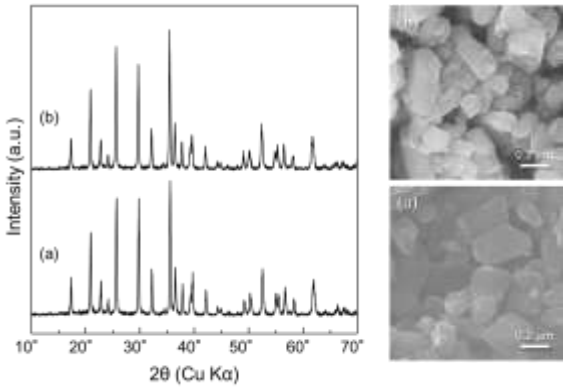

Figure 6. XRD patterns and SEM images of the Mn added products synthesized by hydrothermal process. (a) x=0, and (b)x=0.25.

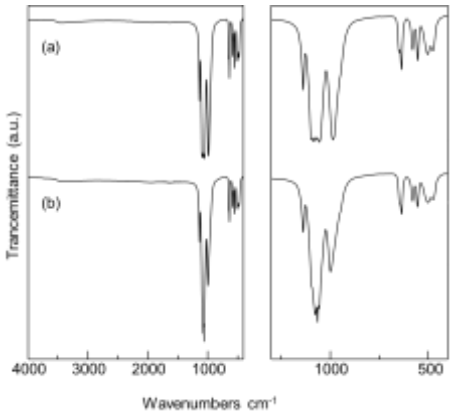

Figure 7. FTIR spectra of the Mn added products synthesized by hydrothermal process. (a) x=0, and (b)x=0.25.

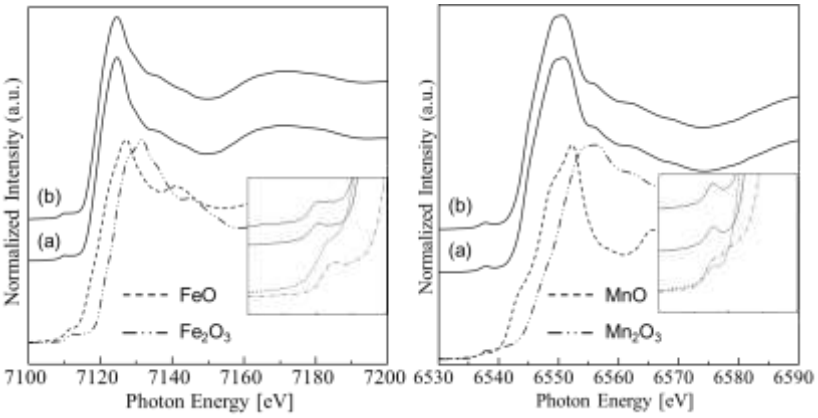

Figure 8. XANES spectra of the Mn added products synthesized by hydrothermal process (a) x=0, and (b)x=0.25.

The Local Structure Analysis

The local structure of transition metal ion, Fe^{2+} and Mn^{2+}, were evaluated by XAFS analysis. XANES spectra of the products synthesized by hydrothermal process were showed in Fig.8. As reference materials, various valent oxides were measured. In Fe *K*-edge XANES spectra of the products, pre-edge peaks attributed to 1s-3d transition was observed at about 7112eV, this is similar to FeO. These results suggested that Fe ion of the products synthesized by hydrothermal process was existed as divalent ion. In the same analysis for Mn *K*-edge, Mn ion was also existed as divalent ion. In addition, the difference between Fe *K*-edge and Mn *K*-edge XANES was not remarkable, so Mn addition was no dependent on coordinal structure or valent for Fe and Mn. From EXAFS analysis. In x=0.25, two radial

distribution function for Fe *K*-edge and Mn *K*-edge were significantly similar, suggesting that Mn was substituted to Fe sites for olivine structure.[19] Therefore, Mn-substituted olivine was successfully synthesized by hydrothermal process.

CONCLUSION

Mn-substituted olivine was successfully synthesized by hydrothermal process. The nano and submicron sized olivines were synthesized under the optimum hydrothermal conditions at 473K for 24h. At the higher temperature, the products has the same olivine structure, but their particle size tended to increase. For the longer hydrothermal reaction time, the particle size of products increased, and their morphologies were plate-like. In the case of Mn addition, the products had olivine structure and the difference of morphology was not remarkable. On the other hands, Mn addition caused the lattice expansion. According to XAFS analysis, Mn ion was existed as MeO_6 octahedral as well as olivines without Mn addition.

REFERENCES

[1] J. Cho, Y. J. Kim, T. J. Kim, B. Park, *Angrew. Chem. Int. Ed.*, **40**, 3367 (2001).
[2] K. Padhi, K. S. Nanjundaswamy and J. B. Goodenough, *J. Electrochem. Soc.*, **144** (1997) 1609.
[3] D. Morgan, A. Van der Ven and G. Ceder, *Electrochemical and Solid-State Letters*, **7 (2)** A30-A32 (2004).
[4] K. Zaghib, A. Mauger, F. Gendron and C. M. Julien, *Chem. Mater.*, **20** (2008) 462.
[5] Kang and G. Ceder, *Nature*, **458** (2009) 190.
[6] J. Barker, M. Y. Saidi and J. L. Swoyer, *Electronchem. Solid-State Lett.*, **6** (2003) A53.
[7] M. Nishijima et.al., *Nature Communications*, **5** (2014) 4553.
[8] K. Padhi, K. S. Nanjundaswamy and J. B. Goodenough, *J. Electrochem. Soc.*, **144** (1997) 1188.
[9] M. Koltypin, D. Aurbach, L. Nazar, B. Ellis, J.Power Sources 174 (2007) 1241.
[10] S. Framger, F. Le Cras, C. Bourbon, H. Rouault, J. Power Sources 119-121 (2003) 252-257.
[11] S. Yang, P.Y. Zavaliji, M. S. Whittingham, *Electrochem. Commun.*, 3 (2001) 505-508.
[12] Yamada, S. C. Chung and K. Hinokuma, J. Electrochem. Soc., **148** (2001) A224.
[13] H. Deng et al. , *Journal of Power Sources*, **220** (2012) 342~347
[14] K. Dokko, S. Koizumi, H. Nakano, and K. Kanamura, *J. Mater. Chem*, **17** (2007) 4803.
[15] Y. Jiang, S. Liao, Z. Liu, G. Xiao, Q. Liu, and H. Song, *J. Mater. Chem. A*, **1** (2013) 4546.
[16] J. Chen and M. S. Whittingham, *Electrochemistry Communications*, **8** (2006) 855-85.
[17] J. Chen et al., *Solid State Ionics*, **178** (2008) 1676-1693.
[18] Rulmont, *Eur. J. Solid Inorg. Chem.*, 1991, **28**, 207.
[19] M. Togo et al. in prepared